

# Novel, Robust, and Versatile Bijels of Nitromethane, Ethanediol, and Colloidal Silica: Capsules, Sub-Ten-Micrometer Domains, and Mechanical Properties

Joe W. Tavacoli,\* Job H. J. Thijssen, Andrew B. Schofield, and Paul S. Clegg

Bicontinuous, interfacially jammed emulsion gels (bijels) are a class of soft solid materials in which interpenetrating domains of two immiscible fluids are stabilized by an interfacial colloidal monolayer. Such structures form through the arrest of the spinodal decomposition of an initially single-phase liquid mixture containing a colloidal suspension. With the use of hexamethyldisilazane, the wetting character of silica colloids, ranging in size and dye content, can be modified for fabricating a novel bijel system comprising the binary liquid ethanediol–nitromethane. Unlike the preceding water–lutidine based system, this bijel is stable at room temperature and its fabrication and resultant manipulation are comparatively straightforward. The new system has facilitated three advancements: firstly, we use sub 100 nm silica particles to stabilize the first bijel made from low molecular weight liquids that has domains smaller than ten micrometers. Secondly, our new and robust bijel permits qualitative rheological work which reveals the bijel to be significantly elastic and self healing whilst its domains are able to break, reform and locally rearrange. Thirdly, we encapsulate the ethanediol–nitromethane bijel in Pickering drops to form novel particle-stabilized bicontinuous multiple emulsions that we christen bijel capsules. These emulsions are stimuli responsive – they liberate their contained materials in response to changes in temperature and solvency, and hence they show potential for controlled release applications.

## 1. Introduction

Structural bicontinuity in soft matter can be found in a number of diverse settings; from cheese to the plumage of birds, where it lends a distinctive texture and adds exotic colors, respectively.<sup>[1,2]</sup> It is also encountered in oil–water surfactant systems when cubic phases (CP) and sponge phases (SP) are formed.<sup>[3–7,8]</sup> Through lattice Boltzmann simulations, it became apparent that a further bicontinuous structure could be fabricated using colloidal particles; namely the bicontinuous interfacially jammed emulsion gel (bijel).<sup>[9,10]</sup> Here, spinodal decomposition (SD) of a binary liquid is arrested because the colloidal particles sequester

to the interface and jam there. A prerequisite for bijel formation is that the colloidal particles display near neutral wetting at the interface to avoid influencing the domain curvature during SD which would promote droplet formation.<sup>[11–13]</sup> The practical realization of the bijel was duly developed by Herzig et al. and it has been proposed that it will have a host of applications, for example, as a micro-fluidic device, used to purify reactions.<sup>[14]</sup> Polymer blends have also been arrested in what appears to be the same mechanism using organo clays, polystyrene drops, carbon black particles and modified silica particles.<sup>[15–18]</sup> Additionally, a bicontinuous structure with interfacially positioned particles has been formed in a phase-separated gelatin–starch water-based solution – but, in this case, particle accumulation at the interface is entropically driven.<sup>[19]</sup>

In essence, the bijel is a Pickering emulsion and though Pickering technology has been previously adapted to hold liquids in some unusual geometries,<sup>[20–22]</sup> the bijel is the first bicontinuous example. Hence, the bijel can be loosely thought of as the particle analogy to the SP. However, apart

from the obvious particle–surfactant difference, two other important distinctions exist. Firstly, unlike the SP and the CP, which form at equilibrium, the bijel is a kinetically arrested structure, maintained only because the particles sit in a deep energy minimum at the interface. The depth of this minimum can be given as

$$E = \pi\gamma R^2 (1 - |\cos \Theta|)^2 \quad (1)$$

where  $R$  is the particle radius,  $\gamma$  is the interfacial tension and  $\Theta$  is the three-phase contact angle of the particle at the interface. The above expression is only strictly valid for an isolated particle on a planar interface.<sup>[23]</sup> The second distinction lies with the size scales involved: bijel domain separations typically lie in the tens of micrometer range whilst those of the SP are nanometer in size.

In the experimental work performed by Herzig et al., two phases of water and lutidine (W and L), which share a lower critical solution temperature, were trapped by silica particles whose wetting was tailored by the addition of fluorescein

Dr J. W. Tavacoli, Dr J. H. J. Thijssen, Dr A. B. Schofield, Dr P. S. Clegg  
School of Physics and Astronomy  
The University of Edinburgh  
Edinburgh, EH9 3JZ, United Kingdom  
E-mail: tavacoli@physics.org

DOI: 10.1002/adfm.201002562

isothiocyanate (FITC) dye (this also rendered the particles fluorescent and resulted in some beautiful images of the bijel) and a rather cumbersome drying protocol.<sup>[11,12,14]</sup> This system has also been used as a template for polymeric, ceramic, and metallic macroporous materials.<sup>[24]</sup> However, this combination of liquids and particles is not ideal as the structure is unstable at room temperature and the tuning of particles is demanding. The difficulties in accessing alternative liquid pairs predominantly lie with controlling the particle wetting because the other requirements of a critical concentration and an appropriate quenching rate are more easily met.<sup>[11,12]</sup>

One way to alter the wetting of silica particles is through the silanization of their surface.<sup>[25]</sup> In this paper we report the reproducible modification of the surface chemistry of silica colloids of varying size and dye content, thereby enabling the introduction of a novel, robust, and versatile bijel system – nitromethane (NM), ethanediol (ED) and silica. This bijel is stable at room temperature and we have used it to make three advancements in bijel technology. Firstly, we have fabricated bijel with domains smaller than ten micrometers by using sub 100 nm silica particles at high concentrations. Secondly, we have made a qualitative exploration of the rheological properties of the bijel and thirdly, we have developed bijel capsules where the bijel is the minority phase in a Pickering emulsion. These capsules are the first example of an encapsulated particle-stabilized bicontinuous architecture and are related to previous research undertaken on multiple Pickering emulsions.<sup>[23,26]</sup> As with conventional Pickering emulsions, the size of the encapsulated and external geometries of our droplets can be controlled through variations in particle concentrations,<sup>[27]</sup> and because the droplets contain two dissimilar liquid domains, they have the capacity to hold chemically distinct materials. In addition, they also have triggered release capabilities because they are sensitive to threshold values in temperature and to solvency effects, and it is plausible that bijel capsule technology may lead to advancements in controlled release.

## 2. Results and Discussion

### 2.1. Sub-Ten-micrometer-Scale Bijels of Nitromethane, Ethanediol, and Silica Particles with Tunable Wettability

Control over the wettability of our particles has laid the foundations for the progress reported in this paper. All bijels presented here are made with Stöber silica that was silanized with the reagent hexamethyldisilazane (HMDS) and we can reproducibly modify our silica colloids. The principal reason why the HMDS based reaction is so robust is because it is carried out in a water, ammonia, and ethanol solution. As a result, the reaction is insensitive to water contamination and the particles are resistant to flocculation: two problems that can plague silanization reactions with (the often used) chlorosilanes.<sup>[28]</sup> As demonstrated in **Figure 1**, the nature of the structure formed after a critical ED–NM phase separation in the presence of silanized silica depends on the wetting properties of the particles because it is only when the three-phase contact angle is close to 90° (Figure 1b) that the curvature of the interface is not affected and a bijel

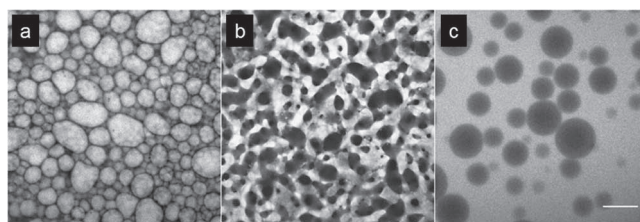


**Figure 1.** The effect of the surface modification of silica particles with HMDS on the emulsions they form after SD. From (a–c) increasing amounts of HMDS were used to silanize the particles. a) Emulsion drops stabilized by the least hydrophobic particles. At the interface these particles predominantly lie in the ED (dark regions) to produce NM (white regions) in ED Pickering emulsions after SD. b) A bijel stabilized with neutrally wetted particles. These particles impart no curvature during spinodal separation and maintain the bicontinuous networks formed during the phase separation. c) Emulsion drops stabilized with the most hydrophobic particles. These particles prefer the NM phase and a ED in NM Pickering emulsion is produced. The scale bar is 100  $\mu\text{m}$ .

is produced. Silica particles modified with too little HMDS (Figure 1a) are favorably wetted by the ED rich phase and bend the interface towards the NM rich phase to produce NM in ED (NM/ED) Pickering drops. The opposite situation is true for particles modified with too much HMDS (Figure 1c) where ED/NM Pickering drops form. We use this relationship to tune the reaction conditions to achieve neutral wetting. For example, if all our HMDS modified silica batches lead to ED/NM Pickering drops, we would surmise that less HMDS is required and the next round of silanization would be tailored accordingly.

**Figure 2** displays confocal micrographs of the ED–NM bijel fabricated using three different silica colloids. Each of these bijels is fully three dimensional (data not shown). The red regions correspond to the NM-rich phase of the bijel which has been rendered fluorescent by the addition of the fluorophore Nile Red and the position of the particles correspond to the tortuous green lines that are clearly visible at the interface. The bijels pictured in Figure 2a and c were fabricated with FITC labelled silica particles, whilst non-dyed silica particles arrested the bijel displayed in Figure 2b. This accounts for

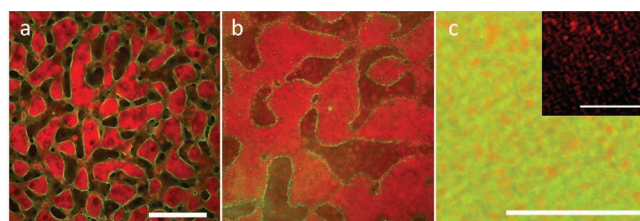


**Figure 2.** Confocal images of ED–NM (dark and red regions respectively) bijels fabricated with different batches of silanized silica (green). The particles can be seen at the liquid–liquid interface. a) and c) Bijels fabricated using FITC tagged silanized silica ( $R = 453$  nm and  $R = 67$  nm respectively). b) A Bijel fabricated with non-fluorescent silanized silica ( $R = 310$  nm). The scale bar in (a) and (b) is 100  $\mu\text{m}$ . The bijel shown in image (c) displays a STMS bijel fabricated with particles at 11.5% volume fraction and both scale bars here are 20  $\mu\text{m}$ . The upper right caption in (c) is an image of the same bijel but with the particle signal removed to highlight the bicontinuous nature of the ED–NM domains. In all images, the double curvature of the domains reflects their near 90° contact angle at the interface.

the notably higher image quality of Figure 2a and c, because fluorescent microscopy was used to collect the particle signals here as opposed to reflection mode for Figure 2b. The domain separations of the bijels vary markedly, with values of 50, 100, and 2.4  $\mu\text{m}$  for Figure 2a, b and c respectively. As detailed in Reference 14, variations in domain size,  $\xi$ , can be described by,

$$\xi \propto \frac{d}{\Phi_v} \quad (2)$$

where  $d$  is particle diameter and  $\Phi_v$  is the volume fraction of the particles.<sup>[27]</sup> The rationale for this relationship is straightforward: a bijel is arrested when all its liquid–liquid interface is covered with particles and small particles and high particle concentrations require more surface area in comparison to large particles and low particle concentrations respectively (for a video of our silanized silica particles trapped at and jamming the liquid–liquid interface to form a bijel see Supplementary Information S1). It then follows from Equation 2 that the average separations in Figure 2a are roughly half that of the separations in Figure 2b because the former shows a bijel made with 453 nm radius silica particles at  $\Phi_v = 3\%$  whilst the latter shows a bijel arrested with 310 nm silica particles at  $\Phi_v = 1\%$ . The bijel presented in Figure 2c has domain separations around 2.4  $\mu\text{m}$  (it should be noted that numerous necks of the bijel have a sub-micrometer width) because it was fabricated with silica with a radius of 67 nm at  $\Phi_v = 11.5\%$ . This sub-tens-micrometer-scale (STMS) bijel is the smallest-scale bijel made to date from low molecular weight liquids.

This is significant because by reducing domain separation by a factor of 20, which is roughly the case here, interfacial area between the separate domains is increased by a factor of 400. Such a large increase in surface area could be useful in a number of instances. For example, it has been proposed that the bijel could act as a microreactor where a reacting solution would be pumped through one set of domains whilst producing products that preferentially diffuse into a counter flowing liquid pumped through the other domain set. In this case, an increase in surface area would improve both the purity and yield of any collected products. Furthermore, the downsizing makes the bijel viable for use in a host of new applications where continuously connected porous media are required. With further work, the size scale reduction will be continued and the ability to control domain size from the micrometer to nano-scale will be employed to tailor the bijel for specific applications.

The ED–NM phase diagram (Figure 3) has a number of features that make it an excellent system for bijel fabrication. Firstly, unlike most binary liquid systems, the ED–NM's phase diagram is highly symmetric and after separation a bicontinuous geometry with two domains of near equal volume is produced. The volume ratio of the liquid phases can be calculated by applying the Lever rule:

$$V_{nm} = \frac{v_c - v_a}{v_b - v_a}, \quad (3)$$

where  $v_c - v_a$  is the length of the tie line from the critical concentration to the ED–NM phase boundary at lower NM concentrations and  $v_b - v_a$  is the width of the phase diagram, and we calculate the ED rich:NM rich volume ratio to be 48:52

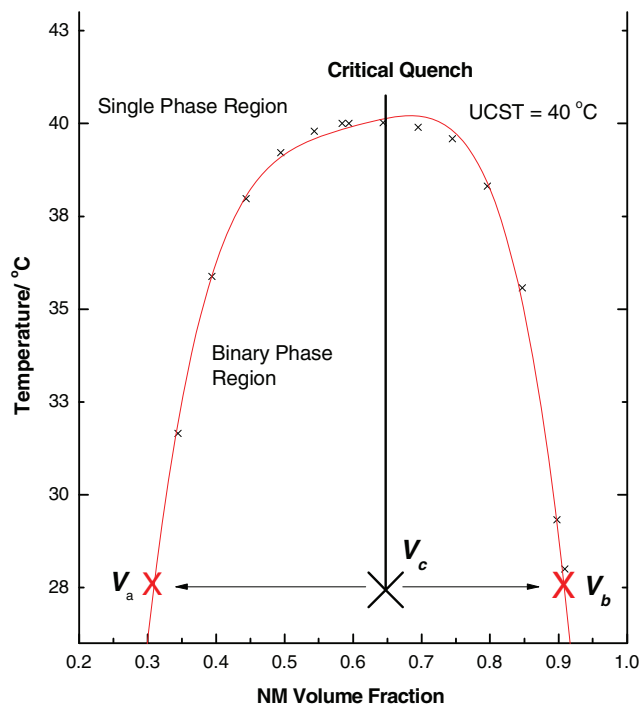


**Figure 3.** The NM–ED phase diagram.<sup>[29]</sup>  $v_c$  denotes the critical concentration,  $v_b$  the NM volume fraction at the NM rich boundary of the phase diagram and  $v_a$  the volume fraction at the ED rich boundary. The liquid–liquid phase diagram is relatively symmetric and phase separation produces two liquid phases of near equal volumes which is ideal for bijel fabrication.

at 26 °C (roughly our quenching temperature). This is supported through inspection of the bijel images in Figure 2 where a pixel count suggests ED:NM volume ratios of 45:55, 44:56 and 49:51 for Figure 2a, b, and c, respectively. These results can be compared to the W:L volume ratio, obtained from the (far more unsymmetrical) W–L phase diagram, of 68.9:31.1. A further advantage is that the ED–NM bijel is not susceptible to gravitational effects such as creaming, because the densities of NM and ED are almost the same (1.13 and 1.11  $\text{g cm}^{-3}$  respectively) and the capillary length is roughly 3 mm at ambient temperature. Storage, transportation and experimentation are far more straightforward because the ED–NM bijel is stable at room temperature and has a UCST of 40 °C (with the presence of particles this is raised to 46.3 °C) and a quench to room temperature is normally sufficient to fabricate the bijel (as explained in the experimental section a quench to 0.5 °C is required for the STMS bijels). This last factor has made our rheological work on the bijel possible because we are able to fabricate the ED–NM bijel in geometries that are more appropriate to the basic experiments outlined in the next section.

## 2.2. Bijel Rheology

Preliminary studies suggested that the bijel has a yield stress through the observation that the sedimentation rate of a cylindrical wire, dropped into a W–L bijel, rapidly fell to zero in the upper regions of the structure.<sup>[14]</sup> Consequently, a lower bound

yield stress of 600 Pa was estimated, though such a large yield stress could be due to van der Waals interactions between particles as it was envisaged that the bijel's static modulus,  $G$ , would scale as

$$G \propto \frac{\gamma}{\xi} \quad (4)$$

i.e., a yield stress 2 orders of magnitude smaller.<sup>[9,13,14]</sup> Just as with Pickering drop distortion, for bijel flow to take place, unjamming of the particle monolayer is required. This requires dilation, and assuming close packing, the minimum yield strain necessary is 0.15.<sup>[30]</sup> However, because the bijel is a fully interconnected structure it is anticipated that significant local flow will only be produced when a larger scale reorganization takes place, i.e., the breaking and reforming of domains. Such reorganization was apparent on the post inspection of the bijel after the aforementioned load bearing experiment. A “healing” effect was also evident because, despite the wire puncturing domains, no interface was left devoid of particles and the configuration of the bijel's domains has been altered to support the wire.<sup>[14]</sup>

Our rheological work involves two simple qualitative experiments that probe the bijel's response to a local, compressional stress and to a shear stress (Figure 4 and Figure 5 respectively). The key feature of this work is that we have been able to visualize the bijel before, during, and after deformation. As demonstrated in Figure 4, when a 120  $\mu\text{m}$  diameter needle is pressed into a ED–NM bijel, contained in an enclosed geometry, a change of length of 5 domains is evident, whilst on relaxation (removal of the needle) the ED–NM bijel resumes a near original state. It is therefore apparent that the bijel is remarkably elastic. The domains adjacent to the needle are observed to elongate during the compression whilst a comparison of Figure 4a with Figure 4h reveals local plastic rearrangement of the areas directly contacted by the needle with the domains here elongated in the axis of the applied compression.

The ‘training’ of the structure seen in the needle compression is more evident in the second rheological test: a simple shear experiment where the ED–NM bijel is first formed between two glass cover slides, after which the top slide is translated with respect to the stationary lower slide (Figure 5). From

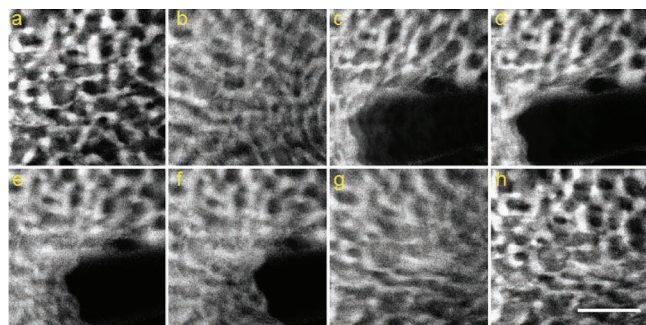


**Figure 4.** a–h) The response of the ED–NM bijel to compression with a nylon needle ( $d_n = 120 \mu\text{m}$ ). Strain of the order of 100  $\mu\text{m}$  (five domain widths) is evident and the bijel resumes a near original state after the removal of the needle. The associated timings are 1.60, 2.40, 2.80, 3.20, 3.40, 4.00, and 5.60 seconds. The bright regions correspond to the ethanol rich phase that was dyed with fluorescein. The scale bar is 100  $\mu\text{m}$ .

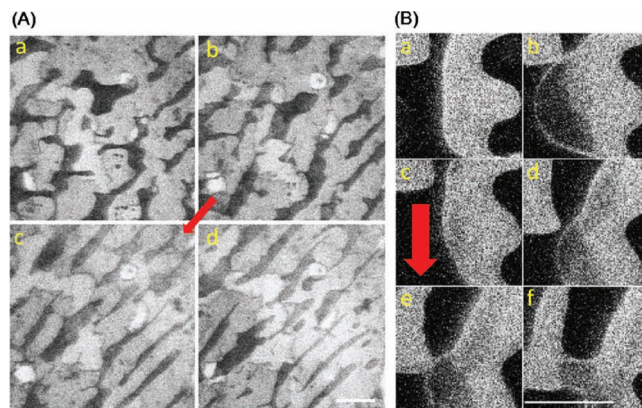


**Figure 5.** The response of a bijel to shear stress. A) (left) a–d) One can clearly see alignment of the domains with the direction of the shear (shear direction is given by the red arrows). No time information is given as the stress was not applied continuously or at an even rate. B) (Right) a–c) The application of shear increases interfacial area leaving areas devoid of particles which snap back into shape as the shear ceases, due to energetically unfavorable liquid–liquid contacts. d–f) If the stretching of a domains takes place close together, domain zipping can occur. Both scale bars are 100  $\mu\text{m}$ .

the separation of domains before and after the deformation, we estimate the strain to be around 25% and the imaging reveals that the bijel is able to modify its architecture in a continuous fashion resulting in an anisotropic final structure whose domains are aligned with the direction of the shear (Figure 5A). The aligning of domains can be compared to simulations by Kim et al. where the bijel orients and thickens in the direction of a force applied at the bijel's interfaces.<sup>[31]</sup> This smooth transition from an isotropic-like structure to anisotropic one requires exceeding the yield stress to allow particle rearrangement at the interface whereupon the bijel is “fluidised” and flows. On relaxation, the bijel returns to a jammed state but one that maintains the imparted orientation. The second part of this concept is illustrated in Figure 5B a–c, as domains can be seen snapping back into a more compact, particle-jammed state to avoid the energetically unfavorable liquid–liquid contacts when shearing momentarily ceases. The bijel is also able to rearrange its connectivity to compensate for the shear stress because separate domains may break and/or coalesce with closely position ones (Figure 5B d–f). Coalescence is possible because the shearing increases the interfacial area of the domains leaving regions devoid of particles. It should be noted that Figure 5B shows a bijel that is one domain deep, roughly 150  $\mu\text{m}$ , whilst the bijel displayed in Figure 5A is around 800  $\mu\text{m}$  in depth and extends upwards by many domains.

These basic compression and shear tests serve to underline the soft–solid nature of the bijel resulting from the connectivity of the domains and confirm some of the speculation about bijel rheology. Furthermore, a fully three-dimensional bijel is a large, arrested analog of the surfactant sponge phase and the results presented here suggest that more ordered arrested phases might be created using “training” in external fields such as shear. Next, we explore the bijel and its structure under confinement. For complete movies of these qualitative rheological experiments please see supplementary materials S2 and S3.

### 2.3. Bijel Capsules

The encapsulation of smaller Pickering drops within larger Pickering drops to form multiple emulsions is a well known method to enclosing two immiscible liquids within the same micro compartment; it is standard practice to achieve this through a step by step liquid addition and mixing procedure.<sup>[26]</sup> We present an alternative to multiple emulsions by fabricating a bijel within a Pickering drop. We christen these novel structures bijel capsules. The host for the capsules is an oil-stabilized silica dispersion in dodecane with a radius of 405 nm (from dynamic light scattering measurements). The dispersion was stabilized through poly-(12-hydroxystearic acid) (PHS) hairs. The bijel capsule's formation route is straightforward, relying on three steps which proceed as follows (for further details see the Experimental section). At 53 °C, a critical ED–NM mixture containing silanized silica particles, is added to this host phase. The resultant mixture (ED, NM, dodecane and two batches of particles) is then hand-shaken to form PHS-silica stabilized Pickering droplets, containing a single phase of ED, NM and silanized silica, within a dodecane continuous phase. To form the bijel capsules, we then quench the mixture to room temperature to induce SD within the drops which is arrested by the silanized silica. The bijel capsules are three dimensionally bicontinuous as seen in **Figure 6** where a characteristic confocal stack is presented. Our results demonstrate that the final location of the different types of particles is determined by their wettability; those with the PHS surface sequester to the outer surface of the capsule (**Figure 6f**), whilst the silanized silica particles remain within the capsule maintaining the internal architecture. Phase separations that take place in confinement are susceptible to boundary effects, for example, it is known that the

preferential wetting of confining walls by one of the two liquids in a binary mixture can alter composition and shift a sample away from criticality.<sup>[32]</sup> Because our temperature quench protocol is relatively slow, any large variations away from the critical concentration would result in nucleation and since we instead observe SD, we infer that pre-transitional wetting has a small effect on the critical phase separation in bijel capsules. The presence of boundaries can also affect liquid–liquid separation by constraining the position, shape and size of domains during de-mixing.<sup>[33]</sup> Again, this effect is minimal, with both the ED and the NM phases sharing the capsule periphery in roughly equal proportions (**Figure 6**) whilst no favored domain orientation is apparent at the boundary.

As currently realized, the external phase of a bijel capsule must be scarcely soluble in both of the internal phases. Hence, the same system can be used to produce droplet-filled capsules, and to switch (i.e., invert) the internal phases by changing the proportions of the two phases.<sup>[22,23]</sup> This catastrophic inversion can be seen in **Figure 7**. To prepare a microcapsule containing a continuous NM-rich phase holding ED-rich droplets (**Figure 7a**), we add an excess of NM relative to the critical composition and perform the mixing, heating and quenching protocol outlined for the bijel droplets. To create a continuous ED-rich phase holding NM-rich droplets (**Figure 7c**), we perform the opposite change in composition. With neutrally wetting particles, inversion takes place at the critical composition (where a bijel forms). In other words, and as observed in **Figure 7**, the internal architecture can be directly related to the phase-separation mechanism: nucleation yields droplets whilst SD yields bicontinuous domains.

As well as controlling the geometry of the structure (i.e., droplets or bicontinuous) we can control the internal channel size within our capsules and the external capsule size as these are inversely proportional to the volume fraction of the silanized silica in the ED–NM phase and the PHS-silica in the dodecane phase respectively (Equation 2). For the capsule diameter, this relationship is presented in supplementary materials S4; control here is loose because the PHS-silica tends to aggregate at higher concentrations and the glass cells (used for visualization purposes) do not allow uniform mixing. For the internal structure presented in **Figure 8**, Equation 2 holds more rigorously and it is evident that there is a reduction in average domain size and an increase in domain tortuosity with an increase in  $\Phi_v$  of the silanized silica particles.<sup>[14]</sup> For sufficiently low  $\Phi_v$  or capsule size, the internal domain size or interface separation begins to become a substantial fraction of the diameter

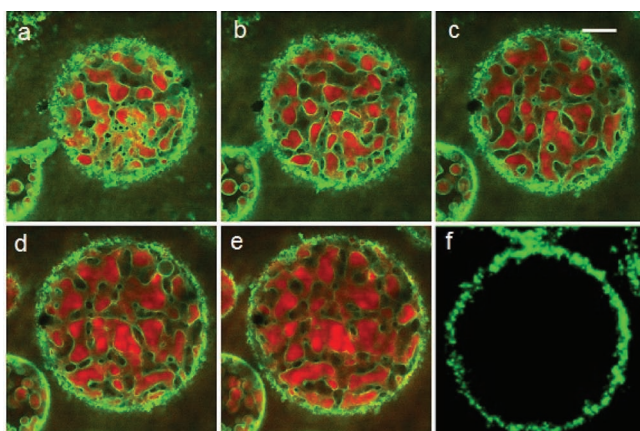


**Figure 6.** a–e) A fluorescent confocal stack of a bijel capsule where the three-dimensional structure of the encapsulated bijel can be clearly seen. The green regions correspond to FITC dyed particles on the interface (silanized silica within the capsule and silica stabilized with PHS chains at the capsule periphery). The ED (dark) and NM (red) rich phase reside within the capsule which sits in a continuous dodecane phase (dark). Images proceed from (a) to (e) and are 10  $\mu\text{m}$  apart, with the lowest image, (e), was taken at 15  $\mu\text{m}$  from the bottom of the sample. The scale bar is 100  $\mu\text{m}$ . f) The isolated fluorescent signal of the PHS-silica particles which stabilize the exterior of the capsules of a capsule whose interior interfaces are populated by non-dyed silica particles.

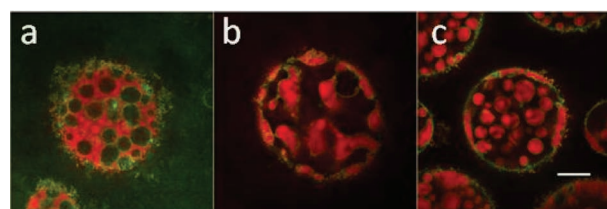


**Figure 7.** a–c) Particle-stabilized multiple emulsions formed after the de-mixing of the binary liquid ED and NM. a) Particle-stabilized droplets of the ED-rich phase contained in a larger drop of the NM-rich phase, b) a bijel and, c) NM-rich droplets contained in a larger ED-rich droplet. The scale bar is 100  $\mu\text{m}$ .

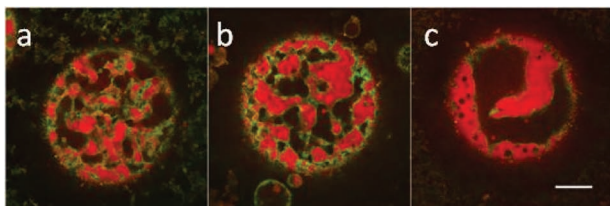


**Figure 8.** Confocal microscopy images showing the effect of  $\Phi_v$  on domain size. a–c)  $\Phi_v = 3.5$ , 2.3 and 1.1, respectively. The color scheme is the same as detailed previously and one can clearly see the reduction of domains size with an increase in  $\Phi_v$ . The scale bar is 100  $\mu\text{m}$ .

of the capsule giving a more open internal architecture. Hence, just as with the bulk bijel, we will be able to tailor capsule size to meet any future application demands.

Note, that there are a variety of areas where it is beneficial to hold two contrasting materials within the same capsule (for example, haircare, where a dye and a bleach are held separately) but released together.<sup>[34]</sup> For such applications we have envisaged three ways that release or mixing might be carried out. Firstly (and most obviously) through the application of shear, just as with vesicle-based delivery vehicles,<sup>[35]</sup> and we have elucidated that for bijel capsules with diameters around 500 nm, that a stress between 40–50 Pa is required to break open the outer particle shell (data not shown). The bijel capsules also have the capacity to release their encapsulated materials through two trigger mechanisms.

The first mechanism is shown in **Figure 9**. Here, the addition of small amounts of ethanol induces partial mixing of all four liquids allowing for the escape of fluorescein dye, contained in the ED phase, into the dodecane. Collapse of the internal architecture is observed because on mixing, interfacial tension, the “glue” that holds the particles at the interface, no longer exists. The second mode of triggered release also relies on removing interfacial tension, achieved this time by heating above the

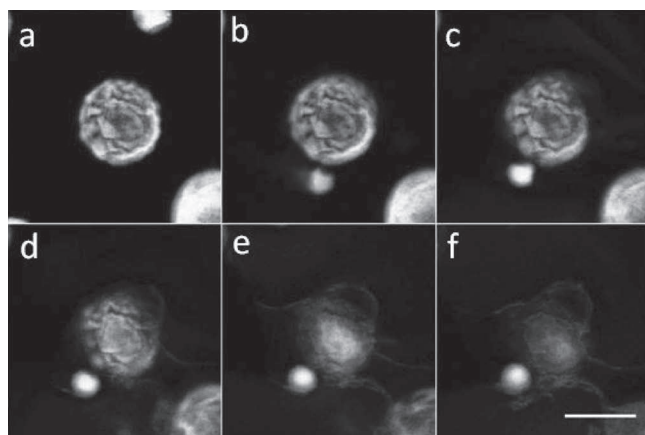


**Figure 9.** a–f) The triggered collapse of a bijel capsule on the addition of ethanol to the continuous dodecane phase. The mixture of ethanol, ED, NM and dodecane is partially soluble, promoting the collapse of the external and internal structure of the bijel and allowing the bulk release of its encapsulated materials. Images were taken one second apart and the scale bar is 100  $\mu\text{m}$ .

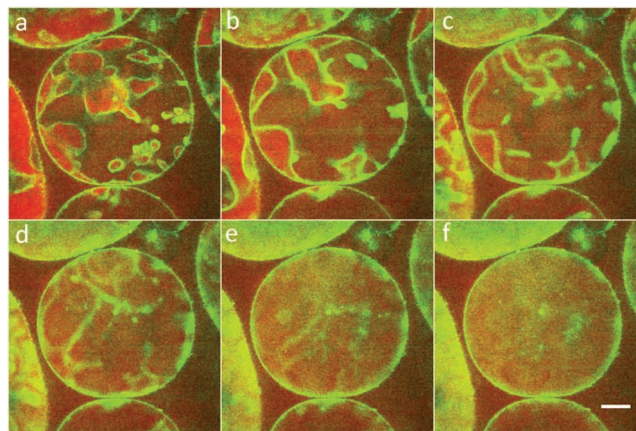


**Figure 10.** a–f) A demonstration of the triggered collapse of the internal particle architecture (caused by liquid remixing). The silica particles (green) are initially at the ED–NM interface. At 46.3 °C, the internal structure collapses, the ED and the NM (red) remix and the particles re-disperse. The heating rate was 17 °C min<sup>−1</sup> and each image was taken 14.4 s apart. The scale bar is 100  $\mu\text{m}$ .

ED–NM UCST of 46.3 °C (with particles). **Figure 10** demonstrates this process and there is a quick collapse of the inner colloidal network during heating and remixing. Whilst the addition of ethanol triggers release of previously encapsulated materials into a continuous phase, this second mechanism only allows internal mixing and does not require the addition of a further material. Because of this, the temperature induced release mechanism could be used to trigger contact and mixing within the capsule between previously compartmentalized reactants. As currently realized, this would be best suited to “large” bodies such as functionalized colloidal particles, that are unable to diffuse through the interstices of the inner colloidal network.<sup>[36]</sup>

### 3. Conclusions

We have prepared bijels from the binary liquid, ethanediol and nitromethane. Silanization has allowed us to make this bijel from a range of silica colloids that vary in size and dye content and the ethanediol–nitromethane bijel has been manipulated to advance knowledge of bijel properties and capabilities. For example, in line with the anticipated scaling behavior, the first bijel with domains smaller than ten micrometers was created by using small silica particles at high concentrations and its comparatively massive surface area broadens the application potential of the bijel. Additionally, the bijel’s mechanical behavior was investigated through the imaging of both uniaxial compression and shear experiments. From the compression experiment, a remarkable elasticity was revealed whilst the shear experiment demonstrated that the bijel domains can be trained with the flow direction. Finally, bijel capsules were formed via spinodal decomposition of the binary liquid within Pickering drops in dodecane where the capsule and the encapsulated domains sizes can be controlled through variations in particle

concentrations. Triggered mixing within the capsules can be achieved by heating above the liquids' upper critical solution temperature whilst the addition of ethanol induces the release of dye into the continuous phase. As such, the bijel capsules concept might find applications in controlled release areas such as in the triggered mixing of flavors required in various food formulations.

#### 4. Experimental Section

**Particle Preparation:** Silica particles were prepared according to the Stöber method or with a slightly modified synthesis for the FITC dyed silica particles.<sup>[37,38]</sup> Silanization of these particles then took place in a solution of hexamethyldisilazane (HMDS), ethanol, water, and ammonia. To prepare the dyed PHS-silica particles that stabilize the bijel capsule surfaces, 3-(trimethoxysilyl) propyl methacrylate was added to a comb polymer made up of a backbone of poly-(methyl methacrylate) and "teeth" of PHS to allow attachment to the silica cores through silane bonds.

**Nitromethane-Ethanediol Bijel and Bijel Capsule Formation:** To make the pre-mixture used for both the bulk bijel and bijel capsules, nitromethane (99 + % Acros Organics) containing the fluorophore Nile Red (Sigma Aldrich) and 1,2-ethanediol (100 + % Sigma Aldrich) were added in critical proportions (mass ratio ethanediol 1:1.75 nitromethane) to the silanized silica. The materials were then mixed for two minutes using a Sonics Vibra-cell set to 5 watts. This process simultaneously dispersed the silica and heated the mixture above the critical temperature to give a single-fluid phase. For bulk bijel formation, the dispersion was then pipetted into a pre-heated (53 °C) optical glass cuvette (Starna Scientific) with a 1 mm path length. For capsule formation, the dispersion was pipetted into a pre-heated glass cuvette containing PHS-silica colloids in dodecane (Sigma Aldrich 99%+) and shaken by hand to form a PHS-silica-stabilized emulsion. In both cases, spinodal decomposition was then initiated by temperature quenching through the critical point. This was achieved either by placing the cuvette in an aluminium block at 23.3 °C, that was specifically designed to fit the cuvette, or by placing them onto a metal surface at room temperature. For the sub-ten-micrometer-scale bijels, after mixing and heating via sonication, the ED, NM and silica mixtures were held at 68.3 °C where they were transferred to pre-heated capillaries (W5010 VitroCom microslides, 0.1 mm × 2.0 mm internal diameters) and then quenched to 0.5 °C using an ice and water mixture.

As outlined above, both the starting temperatures and the quench temperatures were different for the formation of the STMS bijels and standard scale bijels. With regard to the starting temperatures, it was found that for both the STMS and the standard scale bijels, a variety of initial temperatures could be used to produce a stable bicontinuous structure. It therefore appears that the choice of starting temperature does not affect the formation of the final jammed structure (assuming the temperature is above the UCST and below the boiling points of the liquid constituents). However, the depth of the quench is important and the STMS bijels are best formed when quenching to 0.5 °C. An explanation for this requirement can be given when one considers that the depth of the energy minimum at the liquid-liquid interface scales with  $R^2$  (Equation 1). Hence, in the early stages of SD, when the interfacial tension is lowest, smaller particles are more likely to leave the interface than larger ones. Our quench to room temperature may not increase the interfacial tension sufficiently rapidly to hold the smaller particle at the liquid-liquid interface whilst, it is possible, a deeper quench to 0.5 °C does.

**Static Confocal Imaging:** For the "normal"-scale bijels imaging was carried out using a Nikon Eclipse TE300 inverted microscope with a Biorad Radiance 2100 scanner. In all but one example, samples were imaged at 20× magnification with an extra long working distance PlanFluor Nikon objective with an adjustable correction collar. The confocal images of the non-fluorescent silanized-silica particles were obtained using incident light (488 nm) produced by an Ar-ion laser.

Depending on the particle type, light passed through either a D488/10 filter (reflected light) or a HQ515/30 (fluorescent light) before collection. The liquid domains were distinguished by the use of Nile Red or Fluorescein dye, which preferentially partition into the nitromethane-rich and ethanediol phase respectively. The Nile Red dye was imaged using light from a Green Helium-Neon laser (543 nm) and a 570 nm long-pass filter whilst the Fluorescein dye was imaged with the Ar-ion laser and the HQ 515/30 filter as detailed above. The STMS bijels were imaged using a Zeiss Observer Z1 inverted microscope in conjunction with a LSM 700 scanner. A Zeiss 63× objective was used for magnification here.

**Heating and Imaging:** Simultaneous heating and imaging was carried out by fitting a brass resistance heating unit around an aluminum block. The aluminium block was specifically designed to fit the optical cuvettes and has a cylindrical pathway through it to allow visualization of the cuvette. The temperature was controlled by a proportional-integral-derivative controller (Lakeshore 331) with a type-K thermocouple (Omega) positioned at the surface of the glass cuvette. Heating took place at a rate of 17 °C min<sup>-1</sup>.

**Rheological Imaging:** Imaging of the rheological experiments was carried out with a Visitech VTeye confocal scanner connected to a Nikon TE Eclipse 300 inverted microscope which allows for fast acquisition rates. A solid state 488 nm laser was used to excite either the FITC dyed silica or the fluorescein contained in the ethanediol phase. For the compression experiment a 20× extra long working distance PlanFluor Nikon objective was used and the bulk bijel was made as above. For the shear experiment, a NM-ED bijel was made between two glass coverslips and the critical mixture was quenched by direct contact with the room temperature glass slips. A 4× Plan Apo Nikon objective was used for magnification in this case.

#### Supporting Information

Supporting Information is available from the Wiley Online Library or from the author.

#### Acknowledgements

We gratefully acknowledge expert advice from K. White concerning bijel fabrication and we thank Scottish Enterprise (SE/POC/CHM, 8-CHM-003) for financial support. J.H.J.T. is currently a Royal Society of Edinburgh/BP trust Research Fellow.

Received: December 4, 2010  
Published online: May 2, 2011

- [1] J. Kokini, G. van Aken, *Food Hydrocolloids* **2006**, *20*, 438.
- [2] R. O. Prum, E. R. Dufresne, T. Quinn, K. Waters, *J. R. Soc. Interface* **2009**, *6*, S253.
- [3] D. Roux, C. Coulon, M. E. Cates, *J. Phys. Chem.* **1992**, *96*, 4174.
- [4] S. Hyde, Z. Blum, T. Landh, S. Lidin, B. W. Ninham, S. Andersson, K. Larsson, in *The Language of Shape: The Role of Curvature in Condensed Matter: Physics, Chemistry and Biology*, Elsevier, Amsterdam, The Netherlands **1997**, Ch. 5.
- [5] C. J. Drummond, C. Fong, *Curr. Opin. Colloid In.* **1999**, *4*, 449.
- [6] B. J. Boyd, *Int. J. Pharm.*, **2003**, *260*, 239.
- [7] P. T. Spicer, M. L. Lynch, M. Visscher, S. B. Hoath, in *Personal Care Delivery Systems and Formulations*, (Ed: M. Rosen), Noyes Publishing, NorwichNew York, **2003**.
- [8] P. T. Spicer, *Curr. Opin. Colloid Interface Sci.* **2005**, *10*, 274.
- [9] K. Stratford, R. Adhikari, I. Pagonabarraga, J. C. Desplat, M. E. Cates, *Science* **2005**, *309*, 2198.

- [10] E. Kim, K. Stratford, R. Adhikari, M. E. Cates, *Langmuir* **2008**, *24*, 6556.
- [11] K. A. White, A. B. Schofield, B. P. Binks, P. S. Clegg, *J. Phys.-Condens. Mat.* **2008**, *20*, 494223.
- [12] K. A. White, A. B. Schofield, P. Wormald, J. W. Tavaoli, B. Binks, P. S. Clegg, Submitted to *J. Colloid Interface Sci.*
- [13] E. Sanz, K. A. White, P. S. Clegg, M. E. Cates, *Phys. Rev. Lett.* **2009**, *103*, 255502.
- [14] E. M. Herzig, K. A. White, A. B. Schofield, W. C. K. Poon, P. S. Clegg, *Nat. Mat.* **2007**, *6*, 971.
- [15] S. F. Gubbels, R. Jerome, P. Tetssie, E. Vanlathem, R. Deltour, A. Calderone, V. Parente, J. L. Bredas, *Macromolecules* **1994**, *27*, 1972.
- [16] H. Chung, K. Ohno, T. Fukuda, R. J. Composto, *Nan. Lett.* **2005**, *5*, 1878.
- [17] M. Si, T. Araki, H. Ade, A. L. D. Kilcoyne, R. Fisher, J. C. Sokolov, M. H. Rafailovich, *Macromolecules* **2006**, *39*, 4793.
- [18] N. Virgilio, C. Marc-Aurele, B. D. Favis, *Macromolecules* **2009**, *42*, 3405.
- [19] H. Firoozmand, B. S. Murray, E. Dickinson, *Langmuir* **2009**, *25*, 1300.
- [20] A. B. Subramaniam, M. Abkarian, L. Mahadevan, H. A. Stone, *Nature* **2005**, *438*, 930.
- [21] P. S. Clegg, E. M. Herzig, A. B. Schofield, S. U. Egelhaaf, T. S. Horozov, B. P. Binks, M. E. Cates, W. C. K. Poon, *Langmuir* **2007**, *23*, 5984.
- [22] P. S. Clegg, *J. Phys.-Condens. Mat.* **2008**, *20*, 113101.
- [23] R. Aveyard, B. P. Binks, J. H. Clint, *Adv. Colloid Interfac.* **2003**, *100*, 503.
- [24] M. N. Lee, A. Mohraz, *Adv. Mat.* **2010**, *22*, 4836.
- [25] B. P. Binks, T. S. Horozov, *Angew. Chem. Int Edit.* **2005**, *44*, 3722.
- [26] B. P. Binks, A. K. F. Dyab, P. D. I. Fletcher, *Chem. Commun.* **2003**, *20*, 2540.
- [27] S. Arditty, C. P. Whitby, B. P. Binks, V. Schmitt, F. Leal-Calderon, *Euro. Phys. J. E* **2003**, *11*, 273.
- [28] P. Silberzan, L. Leger, D. Ausserre, J. J. Benattar, *Langmuir* **1991**, *7*, 1647.
- [29] J. M. Sørensen, W. Arlt, in *liquid-liquid Equilibrium Data Collection*, (Eds: D. Behrens, R. Eckermann), Vol. 5, Part 1, Dechema, Frankfurt/Main, Germany, **1979**, p. 29.
- [30] A. B. Subramaniam, M. Abkarian, L. Mahadevan, H. A. Stone, *Langmuir*, **2006**, *22*, 10204.
- [31] E. Kim, K. Stratford, M. E. Cates, *Langmuir* **2010**, *26*, 7928.
- [32] B. J. Frisken, F. Ferri, D. S. Cannell, *Phys. Rev. E: Stat., Non-Linear, Soft Matter, Phys.* **1995**, *51*, 5922.
- [33] H. Tanaka, T. Araki, *Europhys. Lett.*, **2000**, *51*, 154.
- [34] J. F. Corbett, *Dyes Pigments* **1999**, *41*, 127.
- [35] H. N. Yow, A. F. Routh, *Soft Matter* **2006**, *2*, 940.
- [36] D. Lee, D. A. Weitz, *Adv. Mater.* **2008**, *20*, 3498.
- [37] W. Stöber, A. Fink, E. Bohn, *J. Colloid. Interf. Sci.* **1968**, *26*, 62.
- [38] A. van Blaaderen, A. Vrij, *Langmuir* **1992**, *8*, 2931.